

# CELL COUNTING OPTICAL PLANAR WAVEGUIDE SENSOR BASED ON (Yb,Nb):RTP/RTP(001) SYSTEM

M. A. Butt <sup>1</sup>, E.S. Kozlova <sup>1,2</sup>, S. N. Khonina <sup>1,2</sup>, R.V. Skidanov <sup>1,2</sup>

<sup>1</sup> Samara State Aerospace University, Samara, Russia

<sup>2</sup> Image Processing Systems Institute Russian Academy of Sciences, Samara, Russia

In this work, we demonstrated metal tagged cell counting based on planar waveguide with the help of a visible light at 633 nm with TM polarization and calculated the output power in relation with the density of cells placed on the waveguide.

**Keywords:** RbTiOPO<sub>4</sub>, (Yb,Nb):RTP/RTP, reactive ion etching, planar waveguide, metal- tagged cell counting.

## Introduction

RbTiOPO<sub>4</sub> (RTP) belongs to KTiOPO<sub>4</sub> (KTP) family of nonlinear optical crystals. These crystals are orthorhombic, with the space group Pna21. These crystals are well known for their large electro-optical coefficients, high nonlinear coefficients and low dielectric constants which make them attractive for electro-optic applications such as modulators and Q-switches [1]. These electro-optic properties makes RTP compounds as attractive material for integrated optical applications for the fabrication of active and passive devices. Traditionally in KTP family, the devices are fabricated by ion diffusion techniques where gradient refractive index contrast is achieved [2]. Planar optical waveguides are already been performed on epitaxial layers (Yb,Nb):RTP on RTP and these systems possess a stepped refractive index contrast, for guiding light in the near infra red (NIR) and visible range. Reactive ion etching (RIE) is widely used for structuring different dielectric materials such as SiO<sub>2</sub> and LiNbO<sub>3</sub>. However, the use of this technique in the KTP family of compounds has been not largely explored.

In the past years, KTiOPO<sub>4</sub> is recognized as a finer material for guiding wave optics. KTP has shown to have attractive properties for SHG of the Nd:YAG and other Nd:doped lasers, sum and difference frequency mixing and optical parametric oscillation processes. KTP thin films offer a practical and cost effective alternative to single crystals with enhanced design and capability for integrated optic applications. Nowadays the literature related to integrated photonics in RTP is scarce as compared to KTP. Over past few years, research has been conducted on RTP in order to explore its properties for the use in integrated photonics. First exploratory research to obtain optimum conditions for RIE in (Yb,Nb):RTP epitaxial layer to obtain a channel waveguide with a height around 1 microns was demonstrated [3]. Recently, some work related to RTP waveguides based on ion exchange, RIE and direct laser writing were demonstrated [4, 5, 6]. We believe that, this report is the first demonstration of the waveguide sensor to count cells based on RTP waveguides.

In this paper, we demonstrated the practical use of (Yb,Nb):RTP/RTP(001) planar waveguide for cell counting based on BeamProp (Rsoft Design Group) simulations. Waveguides are optical structures capable of guiding light by total internal reflection. Waveguides have been

widely used in telecommunication industry for more than 25 years; and were recently employed as a biosensor for detection and diagnosis [7-14]. Generally, in optical waveguides, the electromagnetic field of the guided light extends beyond the waveguide core, known as evanescent field which has been exploited in several ways as sensing mechanism [15-16]. When this evanescent field interacts with the overlaying particles and changes its refractive index, the effective refractive index of the guided mode changes which provides the sensing mechanism. We investigated the effect of evanescent field on the metal tagged objects for sensing purpose as shown in figure 1.

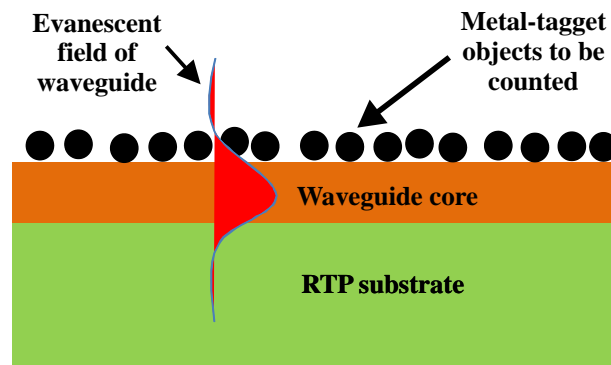


**Fig. 1.** Evanescent wave interacting with the metal tagged objects placed on the top of buried planar waveguide

In our proposed design, we used a planar waveguide of RTP/(Yb,Nb):RTP/RTP(001) system. The design is optimized by varying core and cladding parameters for efficient sensing. In our approach, a visible light of 633 nm TM polarized light as an input, because these waveguides can only guide TM polarization [5]. When the light encounters labeled objects lying above the waveguide, such as cells, the intensity in the waveguide attenuated. The attenuation is proportional to the number of cells placed on the waveguide. There are several practical applications of these waveguides for the biological and chemical sensing [13,17-19]. We have conducted 3-D simulations by using BeamProp software in order to provide the optimized design with high sensitivity.

### Proposed Fabrication Steps

Although this article is based on simulation results of the waveguide sensor, we hereby provide the scheme for the fabrication of such waveguide for future development.

Chromium metal layer deposited on RTP (001) substrate will act as a hard mask during physical etching. Direct laser writing or conventional photolithography is used to provide patterns on positive photoresist. The sample is then developed and chemically etched by commercially available chromium etchant. Now, the sample is ready for RIE. The optimized recipe for etching can be found in [3]. Once, the groove are obtained in the substrate, the epitaxial layer of (Yb,Nb):RTP is grown by using liquid phase epitaxy (LPE) method. The epitaxial layer is polished until it is only present in the groove. The end faces perpendicular to propagation direction are polished and coupled with laser light.

### Analysis of waveguide output power for periodic cell distribution

In this section of the paper, we have analysed the effect of various concentration of cells periodically placed on the waveguide versus the output power for the purpose of cell counting. Three different core heights of 2, 3 and 4  $\mu\text{m}$  are used to examine the sensitivity of the

waveguide sensor. Additionally, we have used a cladding index of 1.35 to represent the aqueous solution that can be expected in the microfluidic channel.

The refractive index of RTP substrate and (Yb,Nb):RTP epitaxial at 633nm was obtained from [5]. To simulate the effect of metal tagged objects, we placed  $4 \times 4 \times 4 \mu\text{m}$  aluminium metal cells and used a complex index of refraction and absorption coefficient of 1.3387 and 7.2975 at 633 nm respectively. The metal coated objects were placed on the waveguide at a distance of 3000  $\mu\text{m}$  from the input of the waveguide till 7000  $\mu\text{m}$  and the total power in the waveguide is analysed. The power stays constant in the waveguide and starts to decrease when encounters the metal coated cells and then remains constant in the absence of the cells. The concentration/number of cells to be placed on the waveguide for the purpose of analysis are calculated according to Table 1.

**Table 1.** The Ratio of Concentration and the Number of Cells to the Total area of placement equalto  $4 \cdot 10^5$  ( $100 \times 4000$ )

Concentration, %	0.01	0.03	0.05	0.07	0.1	0.15
Number	250	750	1250	1750	2500	3750

In order to simulate the propagation along z-axis, we used Implicit Crank-Nicolson scheme with a grid size of 0.4  $\mu\text{m}$  in X, Y and Z and by applying the Simple Transparent Boundary Condition (TBC). The Gaussian pulse was chosen for launch condition. The weight and height of launch field are equal the weight and height of the waveguide core. The cells were periodically placed on a waveguide with a special dynamic array tool by using the formula (1).

$$T_{\text{dist}} = \sqrt{\frac{S_{\text{total}}}{C_{\text{cells}}}}, \quad (1)$$

Where  $T_{\text{dist}}$  is the periodicity of cells,  $S_{\text{total}}$  is the total area which is covered by cells,  $C_{\text{cells}}$  is cell concentration.

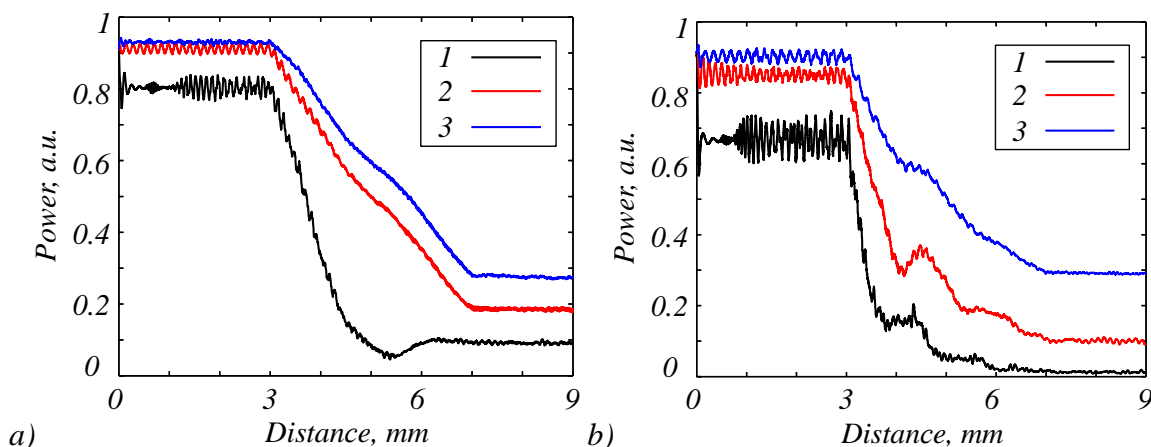


**Fig. 2.** Power vs distance for waveguide with the core thickness of 2 (line 1), 3 (line 2) and 4 (line 3) microns for 5% cells (a) and 15% cells (b).

Figure 2 (a) and (b) represents the power decay versus the propagation distance in the presence of periodic cell distribution placed on waveguide at 5% and 15% respectively. TM polarized light at 633 nm was used for these simulations. It can be seen that, the input power in the waveguide with 2  $\mu\text{m}$  core thickness has some oscillations and has less propagation power as compared to waveguide with core 3 and 4  $\mu\text{m}$  marked in red and blue respectively. It shows

that, core height of 2  $\mu\text{m}$  is not able to support the modes properly at 633 nm. Therefore, we can choose core height of 3 or 4  $\mu\text{m}$  for proper light transmission.

### Analysis of waveguide output power for random cell distribution

We performed some simulations by keeping in mind, the behavior of micro particles placed in aqueous solution over the waveguide. Therefore, we randomly distributed the cells on the cladding layer at a distance of 3000  $\mu\text{m}$  from the input of the waveguide till 7000  $\mu\text{m}$ . These simulations were performed for 1 % of cell concentration with, uniform cell distribution (line 1), random cell distribution (lines 2-5) and various sizes of the cells as explained in Table 2.

Figure 3 shows the power versus distance for the cell concentration of 1 % placed on the waveguide with core height of 3  $\mu\text{m}$ . In case of random (line 2) and uniform cell distribution (line 1), even though, the contact area of cells with waveguide is equal but the sensitivity of the waveguide is much higher for random cells distribution. As the cell size increases, the contact area with the waveguide increases, therefore we can observe a drastic fall of power for 3-5 lines according to their contact areas. The line 5 represents the power decay in the waveguide with larger total volume of the cells ( $V_{\text{total}}$ ) placed on it. The volume of the cells is much larger than other cells distribution under consideration that it can be treated as a cluster of cells placed on the waveguide. But the total area of contact of the cells with the waveguide is equal for line 4 and line 5; therefore, the power decay response is overlapping. This fact suggests that, the cell counting depends on the contact area of the cells with the waveguide.

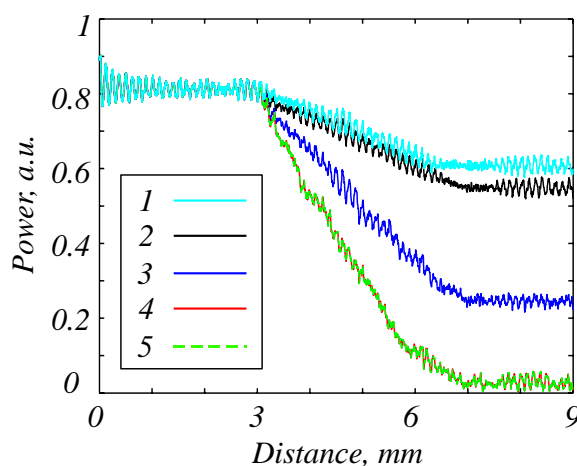


**Fig. 3.** Power vs distance for 1% cells concentrations in case of uniform (line 1) and random (line 2) distribution of cells with the same size, random distribution of cells with different size (line 3-4), random distribution of cluster of cells (line 5)

### Conclusion

In summary, we have proposed a method of using planar buried waveguides based on (Yb,Nb):RTP/RTP(001) system to estimate metal-tagged objects encountering evanescent field of the waveguide. These proposed waveguides can be used for counting metal-tagged cells or other molecules that can scatter energy from the waveguide. The contact area of the cells with the waveguide is the vital factor for cell counting. This technique can work with virtually any metal-tagged cells; we expect this technology to impact on cell counting applications in military medicine, in disaster settings, and in rural healthcare.

**Table 1.** Details of cells distribution used in simulation

№ line	Cell distribution	Cell sizes ( $\mu\text{m}$ )					$S_{\text{total}},$ $\mu\text{m}^2$	$V_{\text{total}},$ $\mu\text{m}^3$
		4x4x4	10x10x4	15x15x15	15x15x4	10x10x10		
1	Uniform	250	-	-	-	-	4000	16000
2	Random	250	-	-	-	-	4000	16000
3	Random	201	49	-	-	-	8116	32464
3	Random	176	-	25	-	49	13342	144639
5	Random	176	49	-	25	-	13342	53364

## Acknowledgements

The work was partially funded by the Russian Federation Ministry of Education and Science, Russian Science Foundation, Presidential grants for support of leading scientific schools and Russian Foundation of Basic Research Grants (14-07-00177, 14-29-07133, 15-07-01174, 15-37-20723, 15-47-02492).

## References

1. Satyanarayan MN, Deepthy A, and Bhat HL. Potassium titanyl phosphate and its isomorphs: growth, properties and applications. *Crit Rev Solid State Mater Sci* 1999, 24(2): 103-91.
2. Risk WP. Fabrication and characterization of planar Ion-exchanged KTiOPO<sub>4</sub> waveguides for frequency doubling. *Appl Phys Lett* 1991, 58(19): 19-21.
3. Choudhary A, Cugat J, Pradeesh K, Sole R, Diaz F, Aguilo M, Chong HMH and Shepherd DP. Single-mode rib waveguides in (Yb,Nb):RbTiOPO<sub>4</sub> by reactive ion etching. *J Phys D: Appl Phys* 2013, 46(14): 145108.
4. Butt MA, Pujol MC, Sole R, Rodenas A, Lifante G, Wilkinson JS, Aguilo M, and Diaz F. Channel waveguides and Mach-Zehnder structures on RbTiOPO<sub>4</sub> by Cs<sup>+</sup> ion exchange. *Optical Material Express* 2015, 5(5): 1183-94.
5. Butt MA, Sole R, Pujol MC, Rodenas A, Lifante G, Choudhary A, Murugan GS, Shepherd DP, Wilkinson JS, Aguilo M, and Diaz F. Fabrication of Y-splitters and Mach-Zehnder Structures on (Yb,Nb):RbTiOPO<sub>4</sub>/RbTiOPO<sub>4</sub> Epitaxial layers by Reactive Ion Etching. *Journal of Lightwave Technology* 2015, 33(9): 1863-71.
6. Butt MA, Nguyen H-D, Rodenas A, Romero C, Moreno P, Vazquez de Aldana JR, Aguilo M, Sole RM, Pujol MC, and Diaz F. Low-repetition rate femtosecond laser writing of optical waveguides in KTP crystals: analysis of anisotropic refractive index changes. *Opt. Express* 2015, 23(12): 15343-55.
7. Huang L, and Guo Z. Biosensing in a microelectrofluidic system using optical whispering-gallery mode spectroscopy. *Biomicrofluidics* 2011, 5: 034114.
8. Li XC, Wu J, Liu AQ, Li ZG, Soew YC, Huang HJ, Xu K, and Lin JT. A liquid waveguide based evanescent wave sensor integrated onto a microfluidic chip. *Appl. Phys. Lett.* 2008, 93: 193901-3.
9. Taitt CR, Anderson GP, and Ligler FS. Evanescent wave Fluorescence biosensors. *Biosens Bioelectron* 2005, 20(12): 2470-87.
10. Xu F, Datta P, Wang H, Gurung S, Hashimoto M, Wei S, Goettert J, McCarley RL, and Soper SA. Polymer microfluidic chips with integrated waveguides for reading microarray. *Anal Chem* 2007, 79(23): 9007-13.
11. Sheridan AK, Stewart G, Ur-Reyman H, Suyal N, and Uttamchandani D. In-Plane Integration of Polymer Microfluidic Channels with Optical waveguides- A Preliminary Investigation. *IEEE Sens J* 2009, 9(12): 1627-32.
12. Myers FB and Lee LP. Innovations in optical microfluidic technologies for point-of-care diagnostics. *Lab Chip* 2008, 8(12): 2015-31.
13. Hofmann O, Voirin G, Niedermann P, and Manz A. Three dimensional microfluidic confinement for efficient sample delivery to biosensor surfaces. Application to immunoassays on planar optical waveguides. *Anal Chem* 2002, 74(20): 5243-50.
14. Burke CS, Stranik O, McEvoy HM, and MacCraith BD. *Optical Chemical Sensors*. Netherlands: Springer, 2006.
15. Garcia D, Ghansah I, LeBlanc J, and Butte MJ. Counting cells with a low-cost integrated microfluidics-waveguide sensor. *Biomicrofluidics* 2012, 6(1): 014115-8.
16. Cunningham BT, and Laing L. Microplate-based, label free detection of biomolecular interactions: applications in proteomics. *Expert Rev Proteomics* 2006, 3(3): 271-81.

17. Friis P, Hoppe K, Leistiko O, Mogensen KB, Hubner J, and Kutter JP. Monolithic integration of microfluidic channels and optical waveguides in silica. *Appl Opt* 2001, 40(36): 6246-51.
18. Puyol M, Salinas I, Garces I, Villuendas F, Llobera A, Dominguez C, and Alonso J. Improved Integrated Waveguide Absorbance Optodes for Ion-Selective Sensing. *Anal Chem* 2002, 74(14): 3354-61.
19. Duveneck GL, Abel AP, Bopp MA, Kresbach GM, and Ehrat M. Planar waveguides for ultra-high sensitivity of the analysis of nucleic acids. *Anal Chim Acta* 2002, 469(1): 49-61.